Deuterium Gas Charging Experiments with Pd Powders for Excess Heat Evolution

(I) Results of absorption experiments using Pd powders

Y. Sasaki[1*], A. Kitamura[1], T. Nohmi[1], Y. Miyoshi[1], A. Taniike[1],

A. Takahashi[2], R. Seto[2], and Y. Fujita[2]

[1]Division of Marine Engineering, Graduate School of Maritime Sciences, Kobe University;

Higashinada-ku, Kobe 6580022, Japan; *088w508w@stu.kobe-u.ac.jp

[2]Technova Inc., Chiyoda-ku, Tokyo 1000011, Japan

A twin system for hydrogen-isotope absorption experiments has been constructed to replicate the phenomenon of heat and ^{4}He generation by D_2 gas absorption in nano-sized Pd powders reported by Arata and Zhang, and to investigate the underlying physics. For Pd·Zr oxide nano-powders, anomalously large energies of hydrogen isotope absorption, 2.4 ±0.2 eV/D-atom and 1.8 ±0.4 eV/H-atom, as well as large loading ratio of D/Pd =1.1 ±0.0 and H/Pd =1.1 ±0.3, respectively, were observed in the phase of deuteride/hydride formation. The sample charged with D_2 also showed significantly positive output energy in the second phase after the deuteride formation. For comparison , results for 0.1- μmφ Pd powder samples and Pd-black samples are also shown.

Introduction

Arata and Zhang recently reported that highly pure D_2 gas charging of Pd nano-powders in the form of Pd/ZrO_2 nano-composite induced significantly higher temperatures inside the reactor vessel than on the outside wall for more than 50 hours, while runs with H_2 gas showed almost no temperature difference.[1] To verify that the excess heat originated in a nuclear process, a QMAS was employed to show the existence of ^{4}He as nuclear ash in the vessel and in the powder after the charging. The charging system is a sophisticated and simplified version of the previous-generation DS reactor[2]. Replication experiments using systems similar to the DS reactor with Pd-black seem to be successful[3,4]. It is extremely important to confirm the phenomenon of heat and ^{4}He generation with fully quantitative confidence.

In the present work we constructed an experimental system to replicate the phenomenon and to investigate the underlying physics. An oxide sample of mixture of Pd (34.6 %) and Zr (65.4 %) was fabricated by Santoku Corporation, Kobe, Japan, and has an average particle size of 7.7 μm, a specific surface area of 37.1 m^2/g, and an average Pd grain size of 10.7 nm. If we assume perfect oxidation of the metal elements, 10 g of the sample contains 3.0 g of Pd.

Experimental system

The D_2/H_2 absorption system is composed of two identical chambers (an A_1·A_2 twin system): one for a D_2 gas foreground run, and the other for H_2 gas background run. As shown in Fig.1 and Fig.2 each part has an inner reaction chamber containing Pd powder and an outer chamber that is evacuated to provide thermal insulation for calorimetry. A sheath heater and a cooling water pipe (copper) are wound on the outer surface of the reaction chamber for baking the sample powder and for flow calorimetry to estimate the heat production rate, respectively. A pair of thermocouples is provided for the flow calorimetry by measuring the temperature difference between the inlet and the outlet of the cooling water.

The D_2 gas is nominally 99.5 % pure and the H_2 is 99.998 % pure. Flow rate control of D_2/H_2 gas purified through a liquid-nitrogen cold trap is made with a Pd membrane filter which also serves as an additional purifier. The Pd membrane (0.2 mm-t, 99.95 %) separates the evacuated reaction chamber (50 mℓ) and the gas reservoir filled with D_2/H_2 at 1 MPa. The gas permeation rate is controllable between 0.1 and 25 sccm by varying the membrane temperature from the room temperature to 900 K. All parameters measured are stored in a PC with an acquisition period of 1 min.
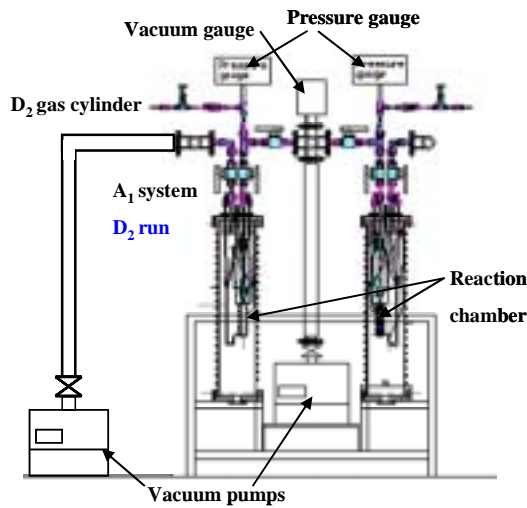

Fig.1. Reduced view of the $A_1 \cdot A_2$ twin system
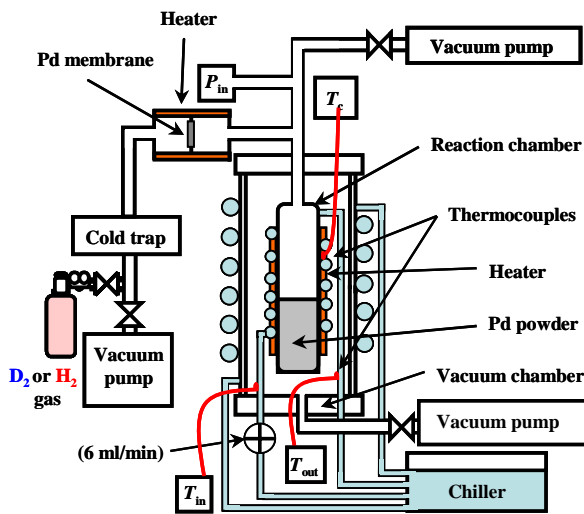

Fig.2. Functional view of A_1

Preliminary experiments

As a calibration of the flow calorimeter, we measured the heat recovery rate under a variety of conditions; with input power of 1, 3, 6 and 10 W, and D_2 gas pressure of 0, 0.1, 0.3 and 1.0 MPa in the reaction chamber. The coolant flow rate was 6 mℓ/min in all cases. The heat recovery rate was found to be almost independent of the pressure and the input power, and the averaged value is (63.1 $\pm$ 5.8) %. Temperature response to a stepwise variation of the input power was found to be expressed as a simple exponential function with a time constant of 5.2 min.

We examined temperature uncertainty and drift, with no sample powder put in the A_1 chamber filled with H_2 gas at a pressure of 1MPa. The inlet-outlet temperature difference and the output power deduced from it showed short-term fluctuation as shown in Fig.3. If we regard an experimental error in the present system as the standard deviation of the longitudinal data, the error or the uncertainty for the output power and the integrated output energy measured for the $A_1 \cdot A_2$ system is evaluated to be 0.014 W and 0.83 kJ for 1000-min acquisition. In the prototype system A_0, which had the larger time constant and smaller sensitivity of heat measurement, and was used in the 1st stage experiments with the 0.1-μmϕ Pd powder and the Pd-black[5], a temperature drift observed sometimes resulted in the
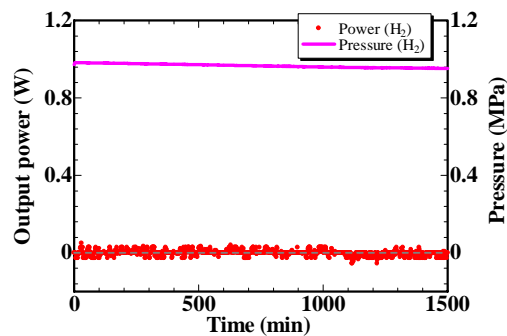

Fig.3. Blank run with no sample powder.

larger error of 4.0 kJ for 1000-min run.

Run number definition

In the following, the run number is designated by "G-PN#M", with G, P, N and M being the gas species, the powder species, powder ID, and the number of repeated use, respectively. The powder species include PP (Pd powder with particle diameter of 0.1 μm and a purity of 99.5 %), PB (Pd-black with a particle size of "300 mesh" and purity of 99.9 %), and PZ (mixed oxides of Pd·Zr). For example, "D-PB2#3" represents the third absorption run with D_2 using a Pd-black sample "2" following evacuation and baking after two cycles of evacuation-baking-absorption.

Results by ϕ0.1μm-Pd powder

First, we describe absorption runs using the A_0 system for five gram of 0.1-μmϕ Pd powder. The reaction chamber filled with the powder was evacuated and heated for baking at 430 K. Then highly pure D_2 or H_2 gas was introduced into the reaction chamber through the Pd membrane filter. The results for the case of D_2 and H_2 absorption are compared in Fig.4. After the gas was introduced, pressure did not begin to rise for a while. During this phase (the first phase) the Pd powder absorbed almost all of the D_2 (H_2) gas atoms as they flowed in, and heat was released as a result of adsorption and formation of deuterides (hydrides). After about 30 minutes, the powder almost stopped absorbing gas; the gas pressure began to rise, and the heat release from deuteride (hydride) formation subsided. This is the beginning of the 2nd phase, and the gas flow rate in the 1st phase is evaluated from the rate of the pressure increase. From the flow rate multiplied by the duration of the 1st phase, loading was estimated to reach $PdD_{0.43}$ ($PdH_{0.44}$).

The output powers are integrated over the 1st phase to give the output energies of 0.10 kJ/g-Pd(D) and 0.08 kJ/g-Pd(H), which are divided by the loading ratio of 0.43 and 0.44 to give the heat of solution ΔH_s of 0.24 eV/atom-D and 0.20 eV/atom-H, respectively. The values appear to be somewhat larger than those found in literatures[6-10]. However, they are consistent with each other, when we take into account that the differential heat of solution is a decreasing function of the loading ratio; ΔH_s = 0.15, 0.12, 0.070, and 0.061 eV/H for H/Pd ratio of 0.5, 0.55, 0.6 and 0.65[9,10]. The difference between D and H, the isotope effect, is rather large, but is not considered to be anomalous, since we find $\Delta H_s(D)/\Delta H_s(H)$ = 1.25 in ref. [9]. On the other hand, the output energies in the 2nd phase, $i.e.$, the output powers integrated over the 2nd phase with duration of 1,400 min, are smaller than the experimental error mentioned above, and "excess heat" is not meaningful in this case. The results are summarized in Table I, which includes those for the Pd-black and the Pd·Zr mixed oxide samples.
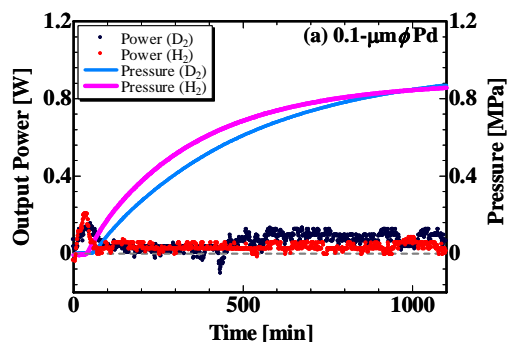

Fig.4. Evolution of heat and pressure in the vessel after introduction of D_2 gas (blue/light blue) or H_2 gas (red/pink) to 0.1-μmϕ Pd powder (D-PP1#1 and H-PP2#1). Power is slightly higher for D than H after 500 min.

Results by Pd-black

The second kind of the sample tested is commercially available 300-mesh Pd-black whose surface has a kind of nano-scale fractal structure finer than the 0.1-μmϕ
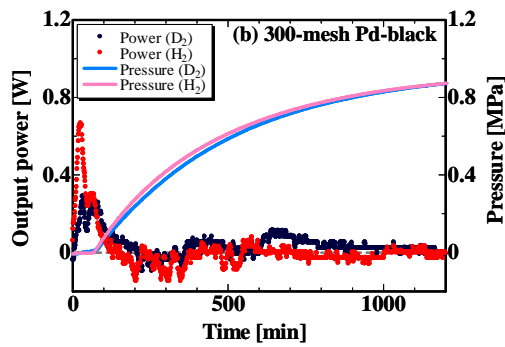
Fig.5. Evolution of heat and pressure in the vessel after introduction of D_2 gas (blue/light blue) or H_2 gas (red/pink) to 300-mesh Pd-black (D-PB1#1 and H-PB2#1). Power is slightly higher for D than H in the 2nd phase.

Pd powder. The performance of Pd-black absorption of D_2 using the A_0 system is compared with that of H_2 in Fig.5. It is very interesting to note that: (1) much higher loading to $PdD_{0.88}$ or $PdH_{0.79}$ is realized, and (2) the output energies in the 1st phase, E_{1st} = (0.67 ±0.12) eV/atom-D and (0.62 ±0.11) eV/atom-H, are 2 - 3 times larger than those for the 0.1-μmϕ Pd powder and those found in the literatures[6-10]. On the other hand, the output energy of 8.3 ± 4.5 kJ (2.6 ± 1.4 kJ/g-Pd) in the 2nd phase of D_2 absorption appears to be larger than that in the case of H_2. The difference is only marginal compared with the above-mentioned error due to the temperature drift of 5.5 kJ in the present case.

Using the improved twin system $A_1 \cdot A_2$, we compared the performance of the Pd-black sample PB3 with a prolonged duration of the 2nd phase of 4,500 min, which was subjected to repeated use with the sample baking before absorption made at 440 K for 3 h (#2), or at 570 K for 1 h (#3). The results are shown in the 6th row through the 8th in Table I.

First we notice that the first run (D-PB3#1) has essentially the same D/Pd ratio and the energy output E_{1st} as those with the A_0 system. Second the repeated use retains almost the same or even higher energy output E_{1st} in spite of the significantly smaller D(H)/Pd ratio. This interesting fact could be related to some
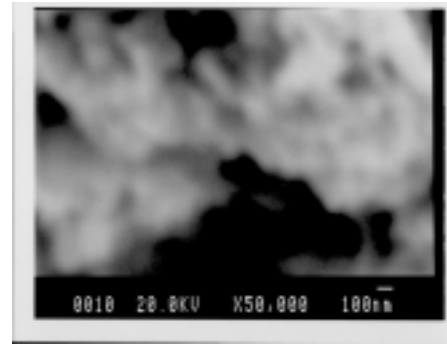

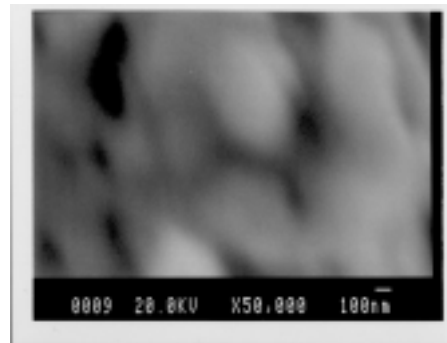Fig.6. SEM photograph of the surface of Pd-black before the absorption run.

Fig.7. SEM photograph of the surface of Pd-black after the absorption run.

structural change of the sample. The SEM photograph of the sample indicated clumping together and disappearance of the fine structure on the scale of several tens of nm. They are shown in Figs. 6 and 7.

As for the 2nd phase, we have little to discuss, when we take into account that they are comparable to the error of 4.0 kJ/1000-min mentioned above for the A_0 system.

Results by Pd-Zr oxide compounds

Now we describe the performance of the mixed oxides of Pd·Zr that are thought to have even finer mesoscopic structure. The results of six runs using virgin PZ samples are summarized in the last 6 rows in Table I. Those of runs with repeated use of the PZ sample will be discussed in the next paper[12] together with the above-mentioned PB samples. Using the $A_1 \cdot A_2$ twin system, the runs H-PZ($2n$)#1 were performed

Table I. Comparison of absorption runs for the 0.1-μmϕ Pd powder (PP), the 300-mesh Pd-black (PB), and the Pd·Zr nano-composite (PZ).

Run #	weight of Pd [g]	Flow rate [sccm]	Output energy [kJ]		Specific output energy [kJ/g]		D/Pd or /Pd (1st ph.)	E1st [eV/D(H)]
			1st phase	2nd phase	1st phase	2nd phase		
D-PP1#1	5.0	2.7	0.5±0.4	2.5±4.1	0.10±0.07	0.52±0.83	0.43	0.26±0.14
D-PP1#2	5.0	3.8	0.5±0.2	4.0±4.4	0.10±0.05	0.79±0.88	0.44	0.25±0.09
H-PP2#1	5.0	5.4	0.4±0.2	2.6±3.9	0.08±0.03	0.53±0.80	0.44	0.20±0.07
D-PB1#1	3.2	3.6	1.7±0.3	8.3±4.5	0.54±0.10	2.60±1.40	0.88	0.67±0.12
H-PB2#1	3.6	4.2	1.6±0.3	(-2.2±4.6)	0.45±0.08	(-0.62±1.30)	0.79	0.62±0.11
D-PB3#1	20.0	2.9	9.3±1.1	1.1±0.5	0.47±0.06	0.06±0.02	0.79	0.65±0.08
D-PB3#2	20.0	0.9	3.3±0.5	3.4±2.6	0.17±0.03	0.17±0.13	0.23	0.79±0.05
H-PB3#3	20.0	2.1	3.2±0.2	14±4.6	0.16±0.01	0.68±0.24	0.24	0.74±0.05
D-PZ1#1	3.0	1.8	7.0±0.2	6.8±1.3	2.33±0.05	2.27±0.43	1.08	2.4±0.05
H-PZ2#1	3.0	2.3	3.6±0.1	(-5.1±1.4)	1.20±0.02	(-1.70±0.47)	1.00	1.3±0.02
D-PZ3#1	3.0	1.9	6.4±0.2	6.2±1.4	2.13±0.05	2.07±0.47	1.08	2.2±0.05
H-PZ4#1	3.0	3.6	4.8±0.1	1.9±1.4	1.60±0.02	0.63±0.47	0.86	2.1±0.03
D-PZ5#1	3.0	2.0	7.1±0.2	1.3±1.4	2.38±0.03	0.42±0.45	1.04	2.5±0.03
H-PZ6#1	3.0	5.9	7.1±0.1	(-0.2±1.4)	2.36±0.02	(-0.08±0.48)	1.34	1.9±0.02
Average for PZ		(D)	6.9±0.4	4.8±3.0	2.3±0.1	1.6±1.0	1.1±0.0	2.4±0.2
		(H)	5.2±1.8	(-1.1±3.6)	1.7±0.6	(-0.4±1.2)	1.1±0.3	1.8±0.4

simultaneously with D-PZ(2n-1)#1, where n = 1, 2, and 3. The A_1 subsystem was used for D-PZ1#1, D-PZ3#1 and H-PZ6#1. In all runs, the PZ sample used was 10 g, and the baking temperature was 570 K for 3 h. The output energy in the 2nd phase is the power integrated over 1,600 min. Examples of the evolution of the output power and the pressure for runs D-PZ1#1 and H-PZ2#1 are shown in Fig.8.

We notice the following four facts in the 1st phase: (1) very large output energies that are more than 3 times greater than those for the Pd-black samples, (2) very large D/Pd (H/PD) ratios of 1.1 ±0.0 (1.1 ±0.3) that are even higher than those for the PB samples, (3) surprisingly large E_{1st} = (2.4 ±0.2) eV (D) and (1.8 ±0.4) eV (H) on the average, and (4) larger isotope effect in E_{1st} compared with those for 0.1-μmϕ powder and Pd-black; the difference just exceeds the error range determined from standard deviations.
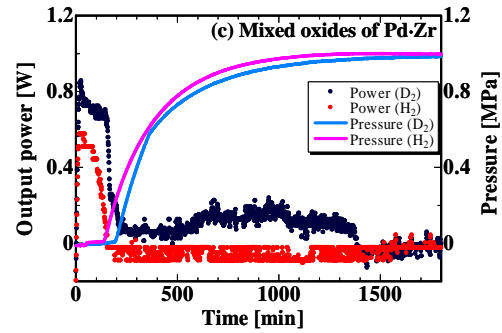
In two runs using H_2, we have negative values for the

Fig.8. Evolution of heat and pressure in the vessel after introduction of D_2 gas (blue/light blue) or H_2 gas (red/pink) to Pd-Zr oxide compounds (D-PZ1#1 and H-PZ2#1). Heat-power level by D is larger than that by H in the 1st phase and also in the 2nd phase.

specific output energy in the rather stable 2nd phase. This should be considered to be due to slight shift in the zero point of the thermocouple signal.

Finally, it should be mentioned that we observed nothing other than steady background in the neutron counter and the scintillation probe located just outside the outer chambers.

More discussions and conclusions on results and underlying physics are given in our succeeding paper[12] in this Proceedings.

References

1) Y. Arata and Y. Zhang: The special report on research project for creation of new energy, J. High Temperature Society, 2008, No. 1.

2) Y. Arata, and Y. Zhang: *Condensed Matter Nuclear Science, Proc. 12th Int. Conf. on Cold Fusion* (ed. A. Takahashi, Y. Iwamura, and K. Ota, World Scientific, 2006) pp.44-54.

3) V. A. Kirkinskii, A. I. Kumelnikov: *Proc. ICCF13, Sochi, 2007* (Publisher Center MATI, Moscow, ISBN 978-5-93271-428-7) pp.43-46.

4) J. P. Biberian and N. Armanet: ibid. pp.170-180.

5) T. Nohmi, Y. Sasaki, T. Yamaguchi, A. Taniike, A. Kitamura, A. Takahashi, R. Seto, and Y. Fujita: http://www.ler-canr.org; to be published in Proc. 14th Int. Conf. Condensed Matter Nuclear Science (ICCF14), Washington DC, 2008.

6) *Hydrogen in Metals II -Topics in Applied Physics*, 29, ed. G. Alefeld and J. Voelkl (Springer, 1978).

7) A. Koiwai, A. Itoh, and T. Hioki: Japan Patent 2005-21860 (P2005-21860A).

8) C. P. Chang, *et al*.: Int. J. Hydrogen Energy, 16 (1991) 491.

9) M. M. Antonova: *Sboistva Gidriedov Metallov* (Properties of Metal-hydrides) (Naukova Dumka, Kiev, 1975; translated by NissoTsushinsha, Wakayama, 1976) [in Japanese].

10) Y. Fukai, K. Tanaka, and H. Uchida: *Hydrogen and Metals* (Uchida Rokakuho, Tokyo, 1998) [in Japanese].

11) H. Fujita: J. High Temperature Society 24 (1998) 272.

12) A. Takahashi, A. Kitamura, T. Nohmi, Y. Sasaki, Y. Miyoshi, A.Taniike, R. Seto, and Y. Fujita: Deuterium Gas Charging Experiments with Pd Powders for Excess Heat Evolution, (II) Discussions on Experimental Results and Underlying Physics, this Proceedings